

H203

Effect of Turbulence on Entrainment of Bubbles by a Plunging Flow

Atsushi SASAKI, Osamu MOCHIZUKI, Masaru KIYA, and Hitoshi ISHIKAWA

Division of Mechanical Science, Graduate School of Engineering, Hokkaido University
N13-W8 Kita-ku Sapporo 060-8628

ABSTRACT The characteristic scales of air bubbles entrained by a vertical thin water-jet plunging into water were investigated to obtain the relation between distributions of bubbles and sounds due to bubbles in a cluster. Distributions of bubbles and the state to the plunging water-jet were observed simultaneously by using a high-speed video camera. The sound was measured by a hydro-phone. It was found that the scaling rule of entrained bubbles and the sound generated by entrained bubbles were strongly affected by the state of the plunging water-jet.

Keywords: Multi-Phase flow, Bubble, Turbulence, Sound, Flow Visualization, Entrainment, Cluster, Turbulent Spot

1. INTRODUCTION

The scaling rule of air bubbles taken into water by a plunging water-jet was studied experimentally in terms of sound generated by bubbles in clusters. The scaling is related to the size and distribution of bubbles as well as clusters. This is an important factor in determining the sound of bubbles. This paper focuses on a relation among the characteristic size and distribution of bubbles, turbulent structures of the flow entraining bubbles and the sound of bubbles.

The entrainment mechanism and dispersion of bubbles by a water-jet plunging into water was investigated by Cummings and Chanson (1997 a, b). They explained the air entrainment process by the instability of a thin air film formed between the plunging water-jet and horizontal water. This instability was discussed by Lezzi and Prosperetti (1991) in terms of the Kelvin-Helmholtz instability applied to the shear layer of a plunging water-jet. The viscosity of water and the difference between speeds of the plunging water-jet and the current in surrounding water were proposed as important factors for determining the bubble entrainment in an ideal condition. However, the other factors affecting the entrainment mechanism in an actual situation are still not clear.

A particular distance between neighboring bubbles as well as clusters was found to exist. In this paper, the characteristic scale of bubbles in relation to scales of fine turbulence and turbulent structures of a plunging water-jet is discussed.

2. EXPERIMENTAL APPARATUS

Typical bubble entrainment can be seen in the region of interaction between a plunging water flow and a stationary water surface. The experimental apparatus used in the present study for observing both the state of a plunging water flow and bubble entrainment is illustrated schematically in Fig. 1. A water-jet along a vertical glass wall was ejected from a nozzle of 1.5 mm in height and 50 mm in width. The distance between the nozzle and the

horizontal stationary water surface was 10 mm. The state of the water-jet was varied by changing the ejection speed V_i from 0.44 to 4.22 m/s. The Reynolds number of the water-jet based on V_i and height of the nozzle ranged from 550 to 5700. The turbulence of the water-jet started to increase as the speed exceeded 0.66 m/s. The speed was estimated from the flow rate measured by a flow meter, and the error in estimation was less than 2%.

The state of the water-jet was determined by the shadow patterns, as seen in the attached picture in Fig. 1 that was taken from behind the vertical wall. We observed three typical patterns: no shadow in a laminar state, intermittent appearance of a spotted shadow in transition from a laminar to turbulent water-jet, and an irregular spotted shadow in a turbulent state. These were judged by shadow patterns correlated to undulation patterns on the surface of the water-jet due to the state of the flow according to the results discussed by Azuma and Hoshino (1984 a, b).

Bubbles entrained near the water surface were observed through the glass wall to investigate the entrainment process and the initial distribution of bubbles.

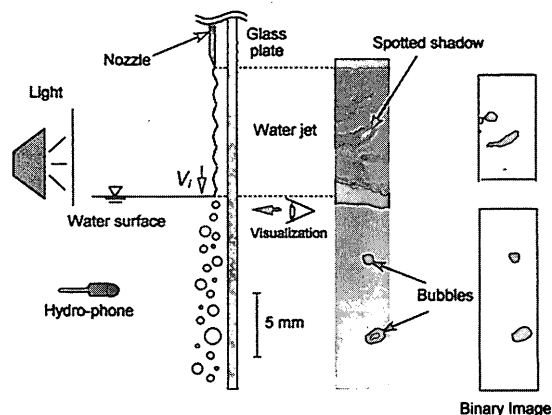


Fig. 1 Schematic sketch showing experimental arrangement and an example of picture and its binary image for observing plunging water-jet and entrained bubbles.

To avoid ambiguity due to disturbances and mixing with bubbles coming to the surface again, bubbles flowing outside the area of observation were discharged through a duct set in the downstream position. Therefore, the data obtained were free from noise caused by ripples generated by bubbles rising to the surface, and it was possible to observe only entrained bubbles.

Distribution of entrained bubbles and flow patterns of the water-jet were simultaneously recorded as shadow graphs using a high-speed video camera. The time interval of each video frame was 1/600 seconds. The video frames were processed by a computer to obtain the radii of bubbles and the distances between neighboring bubbles. To remove noise from a picture, a raw image was transformed into a binary image. An example of a binary image of the flow and bubble patterns is shown in an attached figure in Fig. 1. The area of a shadow and the distance between the centers of neighboring shadows were measured from the binary images. Assuming that a bubble is sphere in shape, the radius of a bubble was calculated from the area of the shadow. The measurement error was within 0.1 mm when the distortion of the lens, determination of the threshold level for a binary image, and the effect of three-dimensionality were taken into account.

The sound emanating from entrained bubbles was measured using a hydro-phone (B&K8103). The measurement position was 10 mm below the horizontal water surface and 10 mm from the vertical wall. Frequency analysis of signatures of sound was performed using a computer. Two hundred spectra were used to obtain an averaged spectrum.

3. RESULTS and DISCUSSION

3.1 Plunging water-jet

The changes in the shadow patterns of the water-jet with different speeds of the plunging water-jet were observed. Typical pictures for each state of the water-jet are shown in Fig. 2. The top edge of the picture is the position of exit of the nozzle, and the bottom edge is the horizontal water-surface. The width of the picture is 4.5 mm.

Azuma et al showed that the surface wave of the film flow was related with turbulence. On the basis of this

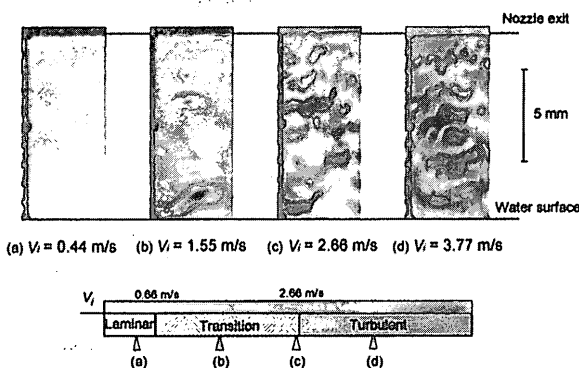


Fig. 2 Change in the state presented by shadow patterns of the plunging water-jet for different speeds. Chart shows the state of each pattern.

result, the turbulence of the water-jet was judged by shadow pattern.

No shadow pattern appeared anytime in the case of $V_i = 0.44$ m/s, as seen in Fig. 2(a). Since the plunging water-jet was laminar, undulations on its water surface did not appear. When the speed was increased, a spotted shadow appeared intermittently. The frequency of appearance was low at $V_i = 1.55$ m/s, as seen in Fig. 2(b). Individual spots showed different degrees of darkness of shadow and different sizes. This state was in the early phase of transition. When the state of flow was in the last phase of transition, the frequency of appearance of a spotted shadow increased, as seen in Fig. 2(c). Clusters of the spotted shadow also increased in this phase. This state seems to be similar to that of turbulent spots in the transition from a laminar to a turbulent boundary layer. The state of the plunging water-jet at $V_i = 3.77$ m/s shown in Fig. 2(d) was turbulent. The boundary between neighboring clusters became vague in this phase. This is similar to the development of a turbulent boundary layer. The individuality of each turbulent spot disappeared in a fully turbulent boundary layer because the spots merged together. According to these similarities, the spotted shadow is regarded as a unit of small-scale turbulence. Though the turbulent intensity of the water-jet was not measured quantitatively in this study, the darkness of the spotted shadow was thought to be associated with the turbulent intensity. A darker/brighter spotted shadow corresponds to a concave/convex surface, as seen in Fig. 1. From the shallow water theory and consideration of continuity, the velocity at the concave part is thought to be greater than that at the convex part. Therefore, the pattern of a spotted shadow shows nonuniformity of local velocity of the plunging water-jet. The correspondence of speed of the plunging water-jet to the state of flow is summarized in an attached chart illustrated in Fig. 2. The spotted shadow appears when the speed of the plunging water-jet exceeded 0.66 m/s.

The characteristic size is obtained as a diameter of a circle with the measured area of the spotted shadow. The change in the diameter d_s with respect to V_i is shown in Fig. 3. The reason why data have dimensions is to compare with data with dimensions for entrained bubbles because of no specific references. The average value of the diameter was almost constant in the tested range, being about 0.6 mm. This means that the scale of fine turbulence of a water-jet is the same order as the height of the water-jet, being independent of speed.

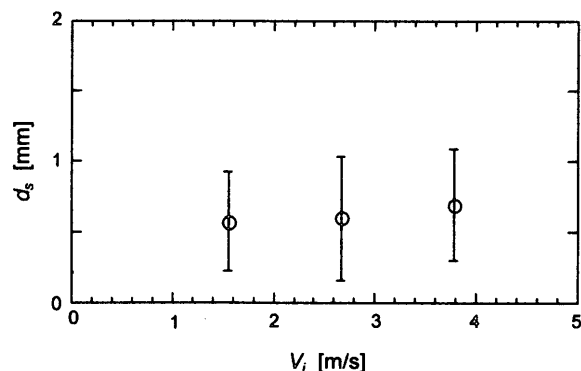


Fig. 3 Change in size of spotted shadow of the plunging water-jet against V_i .

Changes in the distance between neighboring spotted shadows with changes in speed are shown in Fig. 4. Two particular distances were obtained in the cases of $V_i=1.55$ m/s and 2.66 m/s, while one distance prevailed in the case of $V_i=3.77$ m/s. The small distance δ_{s1} is almost constant for each speed, being about 2 mm. This is regarded as the characteristic distance between neighboring small-scale turbulent structures. On the other hand, the larger distance δ_{s2} decreased with increases in speed.

3.2 Entrained bubbles

The distributions of entrained bubbles for different states of the plunging water-jet are shown in Fig. 5. The area of observation is 20mm×5mm. The top edge of the picture was positioned at 7 mm under the horizontal water surface. Clusters of bubbles were seen when the plunging water-jet was in transition, as seen in Fig. 5(a). Bubbles were distributed irregularly in the turbulent case, as seen in Fig. 5(b). These patterns seem to be similar to those of a spotted shadow.

A strong correlation between the state of the plunging water-jet and entrained bubbles is expected from the pictures shown in Fig. 5. To confirm the conjecture, the diameter of bubbles and distance between neighboring bubbles were measured in the same manner as the measurement of those of spotted shadows. The diameters of bubbles for different speeds of the water-jet are shown in

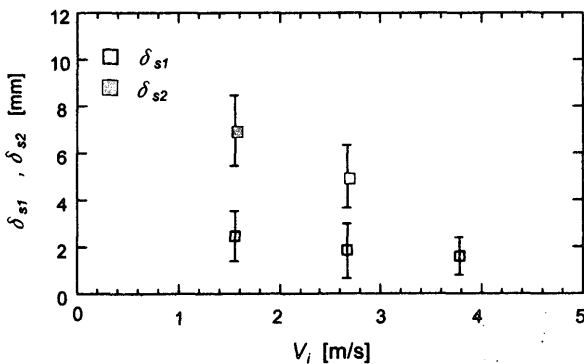


Fig. 4 Change in distance between neighboring spotted shadows of the plunging water-jet against V_i .

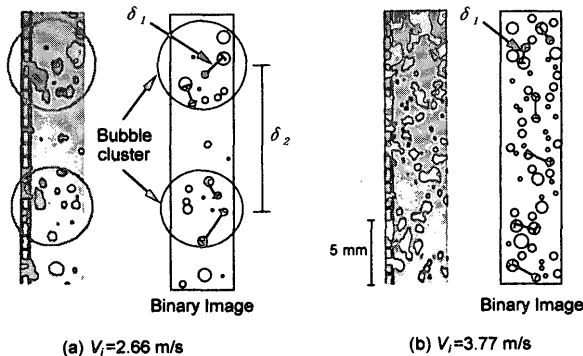


Fig. 5 Characteristic sizes and distances of entrained bubbles for different states of the plunging water-jet. (a) transition state, (b) turbulent state.

Fig. 6. The average diameter for each speed shows a constant value in the tested range, being 0.8 mm. This is close to that of the spotted shadow. This means that the average size of entrained bubbles is determined by the scale of fine turbulence. The deviation is larger than that of the spotted shadow. It is thought that bubbles become large due to coalescence and small by tearing.

The distances between neighboring bubbles are shown in Fig. 7. It is noteworthy that two particular distances appeared in the case of the plunging water-jet in transition, as is seen in Fig. 4. This means that the distribution of bubbles is correlated to that of turbulent structures of the plunging water-jet. The average distances for each are in good agreement with those of the spotted shadow, that is, the characteristic distances of fine-turbulent structures of the plunging water-jet. Accordingly, the relative accurate prediction of the distribution of entrained bubbles is possible if the state of the plunging water-jet is known. This is a remarkable finding in this study.

3.3 Sound generated by bubble clusters

A spectrum of sound generated by bubbles in clusters is shown in Fig. 8. Two particular frequencies, f_1 and f_2 , were observed in the case of the plunging water-jet in transition. The lower frequency, f_1 , was about 4600 Hz and the higher frequency, f_2 , was about 6900 Hz. On the other hand, a dominant peak appeared only at 4500 Hz in the turbulent stage. Since this frequency of 4500 Hz is

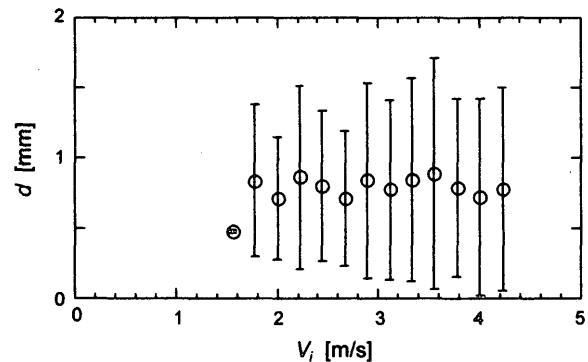


Fig. 6 Change in diameter of entrained bubbles for different V_i .

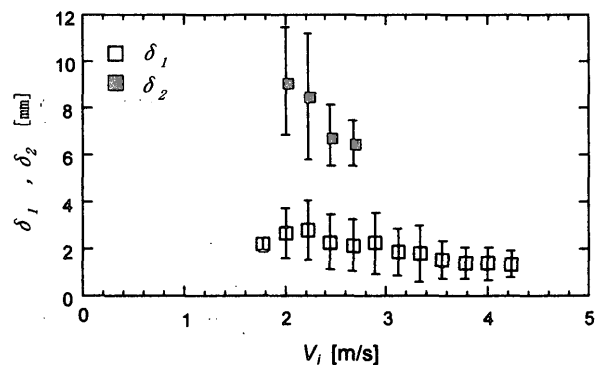


Fig. 7 Change in characteristic distances of entrained bubbles for different V_i .

very close to f_1 in transition, it indicates that there exists a common source of sound in both transition and turbulent states. The common feature is the existence of bubbles with a diameter of 0.8 mm, as seen in Fig. 6. Thus, this is regarded as the sound source with the frequency of f_1 . Supposing that a single bubble with the diameter of 0.8 mm generates sound, the frequency can be calculated by the following equation.

$$f = \frac{1}{\pi d} \sqrt{\frac{3 \gamma P_0}{\rho_w} - \frac{4 \sigma}{\rho_w d}} \quad (1)$$

where $\gamma=1.4$ for air, and ρ_w , σ and P_0 are the density of water, surfactant on the water surface, and pressure inside a bubble, respectively. The calculated frequency is 8200 Hz. This is not in agreement with f_1 or with f_2 . This suggests that a modification that takes the distribution of bubbles into account is needed for estimating the actual frequency.

The oscillation of bubbles with the same diameter in a cluster was analyzed theoretically by Takahira, Akamatsu and Fujikawa (1994). According to their analysis, the natural frequency of bubbles in a cluster was calculated for given δ by the averaged δ_1 ($=1.7\text{mm}$) from Fig. 7. The natural frequency is $f_{m1}=5000$ Hz, as plotted in Fig. 8. This is close to $f_{m1}=4600$ Hz in transition and turbulent states, as seen in Fig. 8. Therefore, this sound is regarded as that of bubbles in a cluster. Supposing that δ_1 is δ_2 ($=6.6$ mm) for the case of $V_i=2.66$ m/s, then the natural frequency is $f_{m2}=6700$ Hz. This is also in good agreement with $f_2=6900$ Hz in the transition state, as seen in Fig. 8 (a). Thus, it is regarded as the sound due to clusters. This sound did not appear in the turbulent case because of no particular distance due to δ_2 in the turbulent state, as seen in Fig. 7. That is, the lower frequency f_1 corresponds to crowded bubbles, while the higher frequency f_2 corresponds

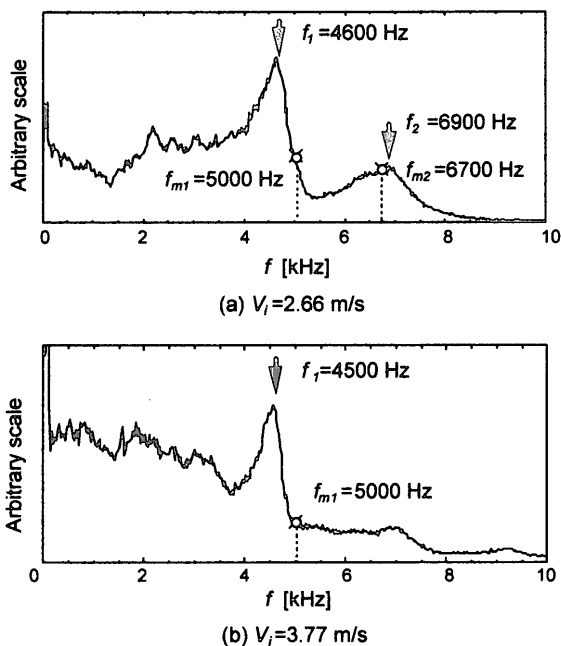


Fig. 8 Spectrum of sound generated by bubbles in clusters. (a) transition state, (b) turbulent state.

to bubbles with the distance between neighboring clusters related to the turbulent spot in the transition state. Sound with f_1 prevails in a turbulent state.

4. CONCLUSIONS

The characteristic scales of air bubbles entrained by a vertical thin water-jet plunging into water was investigated to obtain the relation between distributions of bubbles and sounds due to bubbles in a cluster. Distributions of bubbles and the state to the plunging water-jet were observed simultaneously by using a high-speed video camera. The sound was measured by a hydro-phone. The results indicate that the following relations exist among generated sounds, entrained bubbles and structures in a plunging flow.

The major results are summarized as follows.

- (1) The distribution in size and in distance of the bubbles is strongly affected by the state of the plunging water-jet.
- (2) There are two characteristic distances between entrained bubbles in a transition state: the distance between neighboring bubbles in clusters and the distance between clusters. The scaling rule of entrained bubbles is strongly affected by the state of the plunging water-jet.
- (3) Two particular frequencies of sound are observed in relation to the distance between neighboring bubbles and the distance between neighboring clusters.
- (4) The frequency of sound is completely different from that calculated by vibration of a single bubble in an infinite space. The average diameter of bubbles and the distance between neighboring bubbles was found to be important parameters for estimating the sound of bubbles in a cluster.

5. REFERENCES

1. Azuma, T. and Hoshino, T., The Radial Flow of a Thin Liquid Film (1st Report, Laminar-Turbulent Transition), Bulletin of JSME, Vol. 27 No. 234 (1984 a), pp. 2739-2746.
2. Azuma, T. and Hoshino, T., The Radial Flow of a Thin Liquid Film (2nd Report, Liquid Film Thickness), Bulletin of JSME, Vol. 27 No. 234 (1984 b), pp. 2747-2754.
3. Cummings, P. D. and Chanson, H., Air Entrainment in the Developing Flow Region of Plunging Jets-Part 1 : Theoretical Development, Journal of Fluids Engineering, Sep. Vol. 119 (1997 a), pp. 597 - 602.
4. Cummings, P. D. and Chanson, H., Air Entrainment in the Developing Flow Region of Plunging Jets-Part 2 : Experimental, Journal of Fluids Engineering, Sep. Vol. 119 (1997 b), pp. 603-608.
5. Lezzi, A. M. and Prosperetti, A., The stability of an air film in a liquid flow, J. Fluid Mech., Vol. 226 (1991), pp. 319-347.
6. Takahira, H., Akamatsu, T. and Fujikawa, S., Dynamics of a Cluster of Bubbles in a Liquid (Theoretical Analysis), JSME International Journal, Series B Vol. 37 No. 2 (1994), pp. 297-305.